# Calculation of Site Attenuation From Antenna Factors

ALBERT A. SMITH, JR., SENIOR MEMBER, IEEE, ROBERT F. GERMAN, MEMBER, IEEE, AND JAMES B. PATE, MEMBER, IEEE

*Abstract*—**A site-attenuation model expressed in terms of the antenna factors of the transmit and receive antennas is presented. Both horizontal and vertical polarizations are included, as are the effects of mutual coupling between closely spaced horizontal antennas. Expressing site attenuation in terms of antenna factors allows the use of broad-band antennas with their attendant advantages over tunable dipoles. Measured and calculated results for a variety of sites, antennas, and geometries are compared in the frequency range of 30 MHz to 1 GHz.**

*Key Words*—**Site attenuation, propagation, antennas, antenna factor, test site, open-field.**

## I. INTRODUCTION

SITE attenuation measurements are useful in determining the suitability of test sites for radiated electromagnetic interference and susceptibility measurements. The ideal or reference site is defined as a conducting plane (earth or metal) of infinite extent. Differences between the measured site attenuation on an actual site and the theoretical site attenuation for an ideal site are indicative of site imperfections, such as scatterers in the vicinity of the test antennas, surface roughness, or surface inhomogeneities.

Burrows [1] derived a relation for the attenuation or power transfer between dipoles in free space. Friis [2] later developed simple expressions for the free-space attenuation between arbitrary antennas in terms of power gains and effective apertures. The site attenuation model proposed by the FCC [3] accounts for the ground reflected wave by adding a 4.7-dB average ground reflection factor to the Friis free-space formula. The FCC model is restricted to horizontally polarized tunable dipoles and neglects mutual coupling at close antenna spacings (e.g., 3 m). In addition, the assumption of a 4.7-dB average ground-reflection factor gives inaccurate results below approximately 60 MHz.

The IEC [4] defines site attenuation as the available input power to a short dipole for a field strength of 100 $\mu$V/m at a distance of 3 m over a conducting ground screen. Site attenuation is calculated in terms of the site geometry and the gain and impedance of a standard short dipole. The IEC method precludes the use of most commercial EMC antennas, since their gain and impedance are usually unknown.

Kawana and Miyajima [5], [6] have developed a site attenuation model in terms of the reflection coefficients of the transmitting and receiving antennas which accounts for anten-

Manuscript received May 11, 1981; revised May 27, 1982.

A. A. Smith, Jr., is with the Electromagnetic Compatibility Laboratory, Data Systems Division, International Business Machines Corporation, Poughkeepsie, NY 12602. (914) 463-7726.

R. F. German is with the Electromagnetic Compatibility Laboratory, Information Products Division, International Business Machines Corporation, Boulder, CO 80302. (303) 447-5579.

J. B. Pate is with the Radiation Engineering Laboratory, Communications Products Division, International Business Machines Corporation, Research Triangle Park, NC 27709. (919) 543-6333.

0018-9375/82/0800-0301$00.75 

na-to-antenna and antenna-to-ground-plane mutual coupling. This method is not easily implemented with commercial EMC antennas, since their reflection coefficients are not usually specified.

Bennett and Taggart [7], [8] have proposed a method for characterizing test sites using fixed-height transmitting and receiving antennas. This method eliminates the dependence of results on antenna parameters. However, in contrast with site-attentuation methods which require scanning of the receive antenna height to eliminate nulls, the use of fixed antenna heights exaggerates differences between sites. That is, slight shifts in field-strength nulls between two sites are manifested by large differences in field strength, differences which are completely eliminated by scanning the receiving antenna. The use of fixed antenna heights for site characterization is not consistent with present-day EMC test procedures, which require antenna-height scanning for measurements of products on test sites.

In this paper, we develop a site attenuation model expressed in terms of the antenna factors of the transmit and receive antennas, and a field-strength term readily calculated from classical ground-wave propagation theory. (Antenna factors are usually supplied by the manufacturers of EMC antennas.) Both horizontal and vertical polarizations are included. The effects of mutual coupling between closely spaced horizontal tunable dipoles are accounted for by an antenna-factor correction term calculated from the mutual impedances of the antennas. Since site attenuation is given directly in terms of antenna factors, measurements can be made with broad-band antennas with their attendant advantages over tuned dipoles (e.g., reduced measurement time, compatibility with modern automated EMC instrumentation, and lower mutual coupling).

The model is developed in the following section; measurement procedures are described in Section III. A comparison of measured and calculated results is given in Section IV.

## II. SITE-ATTENUATION MODEL

### A. Receiving Antenna

The equivalent circuit of a receiving antenna system is shown in Fig. 1. $V_{oc}$ is the open-circuit voltage induced by the incident electric field $E$, $h$ is the effective height (or effective length), and $Z_A$ is the antenna impedance. $V_R$ is the voltage received by the 50-Ω field-strength meter. All balun, cable, attenuator, matching-network losses, etc., are indicated in the box in Fig. 1.

By definition

$$V_R = \frac{E}{AF_R} \tag{1}$$

where $AF_R$ is the antenna factor of the receiving antenna. Note that all the parameters of the receiving antenna system (effective height, antenna impedance, and losses) are embedded in the antenna factor defined by (1).

### B. Transmitting Antenna

Fig. 2 shows the equivalent circuit of a transmitting antenna system. The 50-Ω source (signal generator) has an open-circuit voltage $V$. $R_A$ is the antenna resistance (equal to the radiation resistance, since the antenna is assumed lossless), $X_A$ is the antenna reactance, and $I$ is the antenna current. Again, all balun, cable, attenuator, matching-network losses, etc. are relegated to the box in Fig. 2.

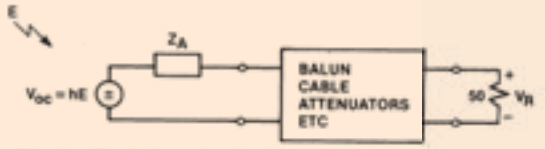


Fig. 1. Equivalent circuit of a receiving antenna system.

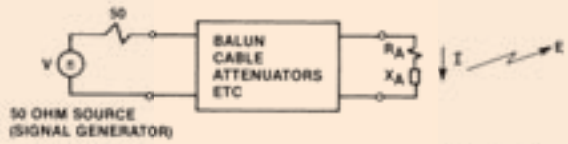


Fig. 2. Equivalent circuit of a transmitting antenna system.

For any transmitting antenna, the free-space far-field electric field strength $E$ at a distance $d$ is [9]

$$E = \frac{(30P_TG)^{1/2}}{d}\, e^{-j\beta d} \tag{2}$$

where

$P_T$ radiated power,
$G$ antenna gain,
$\beta$ $2\pi/\lambda$, free-space wavenumber (phase constant),
$\lambda$ wavelength.

But

$$P_T = I^2R_A.$$

Then

$$E = \frac{I(30R_AG)^{1/2}}{d}\, e^{-j\beta d}. \tag{3}$$

As shown in Appendix I, the reciprocity theorem can be used to express the antenna current of the transmitting antenna in terms of the antenna factor. (The antenna factor of the transmitting antenna $AF_T$ is just the usual antenna factor defined as $AF = E/V_R$ when the antenna is used for reception.) The result is

$$I = \frac{V}{50AF_T}\,\frac{\pi}{\lambda}\left(\frac{120}{GR_A}\right)^{1/2}. \tag{4}$$

Substituting (4) in (3) yields

$$E = \frac{V\pi(120 \times 30)^{1/2}}{50AF_T\lambda}\,\frac{e^{-j\beta d}}{d}.$$

Finally, using $\lambda = 300/f_M$, the free-space far-field electric

field strength $E$ at a distance $d$ meters can be written

$$E = \frac{Vf_M}{79.58AF_T}\frac{e^{-j\beta d}}{d} \tag{5}$$

where

$V$ open-circuit voltage of the 50-Ω signal source,
$AF_T$ antenna factor of the transmitting antenna,
$f_M$ frequency, in megahertz.

*C. Ground Wave, Horizontal Polarization*

Since the surface-wave component of the horizontal ground wave can be neglected above 30 MHz, the electric field radiated by a horizontal dipole antenna over a ground plane with reflection coefficient $\rho_h = |\rho_h|e^{j\Phi_h}$ is just the sum of the direct and ground-reflected waves. Using the expression for the free-space field in (5) and the geometry in Fig. 3, we have

$$E_H = \frac{Vf_M}{79.58AF_T}\left[\frac{e^{-j\beta d_1}}{d_1} + \frac{|\rho_h|e^{-j\beta d_2}e^{j\Phi_h}}{d_2}\right]. \tag{6}$$

In general, the first and second terms of (6) must be modified to account for the pattern directivity of high-gain antennas (e.g., microwave horns). The method is the same as that discussed below for vertical antennas. However, this modification has not proved necessary for the type of broad-band EMC antennas commonly used below 1 GHz (e.g., biconicals, log planar dipole arrays, etc.), which have gains only in the order of 6 dB.

The magnitude of (6) is

$$E_H = \frac{Vf_M}{79.58AF_T}\frac{[d_2^2 + d_1^2|\rho_h|^2 + 2d_1d_2|\rho_h|\cos(\phi_h - \beta[d_2 - d_1])]^{1/2}}{d_1d_2}. \tag{7}$$

For convenience, define

$$E_{DH} = \frac{\sqrt{49.2}\,[d_2^2 + d_1^2|\rho_h|^2 + 2d_1d_2|\rho_h|\cos(\phi_h - \beta[d_2 - d_1])]^{1/2}}{d_1d_2} \tag{8}$$

where

$$d_1 = [R^2 + (h_1 - h_2)^2]^{1/2}$$
$$d_2 = [R^2 + (h_1 + h_2)^2]^{1/2}$$
$$\rho_h = \frac{\sin\gamma - (K - j60\lambda\sigma - \cos^2\gamma)^{1/2}}{\sin\gamma + (K - j60\lambda\sigma - \cos^2\gamma)^{1/2}} \text{ (see [9])}$$

$K$ relative dielectric constant,
$\sigma$ conductivity, in siemens/meter.

$E_{DH}$ in (8) is just the ground-wave electric field strength in microvolts/meter for a horizontal half-wave dipole with one picowatt of radiated power. In (8), $(49.2)^{1/2}$ derives from (2) with $P_T = 1$ pW and $G = 1.64$ (the gain of a half-wave dipole). In calculating site attenuation, the maximum value of (8) in the receiving-antenna height-scan range $h_2^{\min} \leq h_2 \leq h_2^{\max}$ must be computed. (This range may or may not contain the peak field.) Denote this as $E_{DH}^{\max}$. Then the horizontal electric field strength over a ground plane from (7) and (8), maximized over the height-scan range $h_2^{\min} \leq h_2 \leq h_2^{\max}$, is

$$E_H^{\max} = \frac{Vf_M E_{DH}^{\max}}{79.58AF_T\sqrt{49.2}}. \tag{9}$$

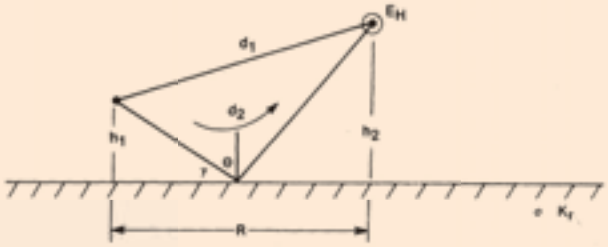


Fig. 3. Propagation geometry for horizontal polarization.

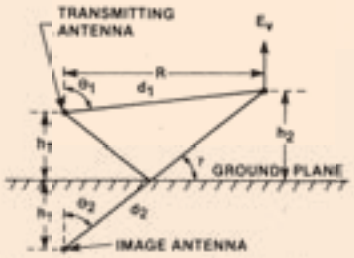


Fig. 4. Geometry for vertical site attenuation.

*D. Ground Wave, Vertical Polarization*

The surface-wave component of the vertical ground wave may be neglected for frequencies above 30 MHz, and the surfaces and geometries normally used for site attenuation measurements (e.g., over a conducting ground, and over an earth plane for antenna heights used for site attenuation measurements). For a vertical transmitting antenna over a ground plane as shown in Fig. 4, (6) must be modified to account for directivity. If $F(\Theta)$ is the directivity pattern, the vertical component of the electric field can be written

$$E_V = \frac{Vf_M}{79.58AF_T}\left[\frac{e^{-j\beta d_1}}{d_1}F(\Theta_1)\sin\theta_1 + \frac{|\rho_V|e^{-j\beta d_2}e^{j\Phi_V}}{d_2}F(\Theta_2)\sin\theta_2\right] \tag{10}$$

where the vertical reflection coefficient is given by [9] as

$$\rho_V = \frac{(K - j60\lambda\sigma)\sin\gamma - (K - j60\lambda\sigma - \cos^2\gamma)^{1/2}}{(K - j60\lambda\sigma)\sin\gamma + (K - j60\lambda\sigma - \cos^2\gamma)^{1/2}}.$$

For electrically short dipole antennas, $F(\theta) = \sin\theta$. This directivity pattern can also be used with little error for the type of EMC antennas used for site-attenuation measurements below 1 GHz (e.g., tuned dipoles, biconical dipoles, and log planar dipole arrays). Since

$$\sin\Theta_1 = \frac{R}{d_1}$$

and

$$\sin\Theta_2 = \frac{R}{d_2}$$

we have from (10)

$$E_V = \frac{Vf_M}{79.58AF_T}\left[\frac{R^2 e^{-j\beta d_1}}{{d_1}^3} + \frac{R^2|\rho_V|e^{-j\beta d_2}e^{j\phi_V}}{{d_2}^3}\right]. \quad (11)$$

Taking the magnitude of (11) yields

$$E_V = \frac{Vf_M}{79.58AF_T}\frac{R^2[{d_2}^6 + {d_1}^6|\rho_V|^2 + 2{d_1}^3{d_2}^3|\rho_V|\cos(\phi_V - \beta[d_2 - d_1])]^{1/2}}{{d_1}^3{d_2}^3} \quad (12)$$

As before, we define $E_{DV}$ as the ground-wave electric field strength in microvolts per meter for a vertical half-wave dipole with 1 pW of radiated power, i.e.,

$$E_{DV} = \frac{\sqrt{49.2}R^2[{d_2}^6 + {d_1}^6|\rho_V|^2 + 2{d_1}^3{d_2}^3|\rho_V|\cos(\phi_V - \beta[d_2 - d_1])]^{1/2}}{{d_1}^3{d_2}^3} \quad (13)$$

where $(49.2)^{1/2}$ derives from (2) with $P_T = 1$ pW and $G = 1.64$. For site-attenuation calculations, the maximum value of (13) must be computed in the receiving-antenna height-scan range ${h_2}^{\min} \leq h_2 \leq {h_2}^{\max}$. If this is denoted as ${E_{DV}}^{\max}$, then the vertical electric field strength over a ground plane from (12) and (13), maximized over the height-scan range $h_2$, is

$${E_V}^{\max} = \frac{Vf_M{E_{DV}}^{\max}}{79.58AF_T\sqrt{49.2}} \quad (14)$$

which is analogous to (9) for horizontal polarization.

*E. Site Attenuation*

A convenient choice for the definition of site attenuation $A$ (and the same one chosen by Kawana and Miyajima [5]) is

$$A = \frac{V_I}{V_R} \quad (15a)$$

or

$$A\ (\text{dB}) = V_I\ (\text{dB}\cdot\mu\text{V}) - V_R\ (\text{dB}\cdot\mu\text{V}) \quad (15b)$$

where

$V_I$ the indicated signal-generator voltage (i.e., dial reading),

$V_R$ the received voltage measured with a field-strength meter or spectrum analyzer.

Equations (15a), (15b) define site attenuation in terms of easily accessible measurement quantities: the signal-generator reading and the field-strength-meter reading.

Since $V = 2V_I$ (i.e., the open-circuit voltage of a signal generator is twice the matched output, or indicated, voltage), (15a) can be rewritten as

$$A = \frac{V}{2V_R}. \quad (16)$$

Substituting (1) into (16) yields

$$A = \frac{VAF_R}{2E}. \quad (17)$$

Finally, substituting (9) or (14) into (17) gives the desired form for the theoretical site attenuation in terms of antenna factors:

$$A = \frac{79.58AF_RAF_T\sqrt{49.2}}{2f_M{E_D}^{\max}}$$

or

$$A = \frac{279.1AF_RAF_T}{f_M{E_D}^{\max}} \quad (18)$$

In decibels

$$A\ (\text{dB}) = -20\log f_M + 48.92 + AF_R\ (\text{dB/m}) + AF_T\ (\text{dB/m}) - {E_D}^{\max}\ (\text{dB}\cdot\mu\text{V/m}) \quad (19)$$

where

$f_M$ frequency, in megahertz,

$AF_R$(dB/m) antenna factor of receiving antenna, in decibels/meter,

$AF_T$(dB/m) antenna factor of transmitting antenna, in decibels/meter,

$E_D{}^{max}$(dB·μV/m) maximum electric field in receiving-antenna height-scan range $h_2{}^{min} \leq h_2 \leq h_2{}^{max}$ from a theoretical half-wave dipole with 1 pW of radiated power computed from (8) for horizontal polarization and from (13) for vertical polarization. (See Appendix III for tabulations of $E_D{}^{max}$ for some typical geometries.)

Cable losses can be handled in two ways. They can be subtracted from the measured site-attenuation data or added to the theoretical site attenuation. Both methods are equivalent (and both are used in this paper), but the former is preferred since site-attenuation data obtained with different cables (but the same antennas) can be compared directly without the need to subtract cable losses. The former method also offers advantages when using automatic spectrum analyzers, since the cable loss, stored in a separate data register, can be subtracted automatically from the measured site-attenuation spectrum. The form in (19) is used when cable losses are subtracted from the measured data. When cable losses are not subtracted from the measured data, they must be added to (19), viz.,

$$A\,(\mathrm{dB}) = -20\log f_M + 48.92 + AF_R\,(\mathrm{dB/m}) + AF_T\,(\mathrm{dB/m}) - E_D{}^{max}\,(\mathrm{dB}\cdot\mu\mathrm{V/m}) + C_A\,(\mathrm{dB}) \tag{20}$$

where $C_A$(dB) is the total cable loss (transmit and receive cables), in decibels.

It will now be shown that, for horizontally polarized matched resonant dipoles and an assumed value of 4.7 dB (1.718) for the "average ground-reflected component," (20) reduces identically to the site-attenuation equation given in FCC Bulletin OCE 44 [3]. Under the FCC ground-reflection assumption, (8) reduces to

$$E_{DH}{}^{max} = 1.718\,\frac{\sqrt{49.2}}{D}$$

or

$$E_{DH}{}^{max}\,(\mathrm{dB}\cdot\mu\mathrm{V/m}) = 21.62 - 20\log D \tag{21}$$

where $D$ is the distance in meters between transmitting and receiving antennas.

Also, it can be shown that the antenna factor for a resonant dipole terminated in (or driven from) 50 Ω through a matching balun transformer with a turns ratio of

$$N = (73/50)^{1/2}$$

is just

$$AF = \frac{2\pi}{300}\,(73/50)^{1/2} f_M$$

or

$$AF\,(\mathrm{dB}) = 20\log f_M - 31.94. \tag{22}$$

Substituting (21) and (22) into (20) yields

$$A\,(\mathrm{dB}) = -20\log f_M + 48.92 + 2(20\log f_M - 31.94) - (21.62 - 20\log D) + C_A$$

or

$$A\,(\mathrm{dB}) = 20\log f_M + 20\log D - 36.6 + C_A \tag{23}$$

which is identical to the equation in OCE 44 for resonant dipoles ($G = 2.15$ dB).

### *F. Mutual Impedance*

There is ample evidence that site attenuation measurements for closely spaced (e.g., 3 m) horizontally polarized antennas exhibit antenna-to-antenna and antenna-to-ground-plane mutual coupling below approximately 100 MHz. For example, see [6]. This is especially true for tunable dipoles at or near resonance.

The antenna terminal impedance change due to close proximity coupling between the transmit and receive dipole antennas as well as the antenna-to-ground-plane coupling can be modeled using a two-port voltage model [6]. We have (see Fig. 5)

$$V_1 = I_1 Z_{11} + I_2 Z_{12} + I_3 Z_{13} + I_4 Z_{14} \tag{24}$$

$$V_2 = I_1 Z_{21} + I_2 Z_{22} + I_3 Z_{23} + I_4 Z_{24} \tag{25}$$

where

$Z_{11}$ self-impedance of antenna 1,

$Z_{22}$ self-impedance of antenna 2.

Define

$E_{mn}(Z)$ electric field at antenna $m$ due to current $I_n$ along antenna $n$,

$I_n(0)$ current at input of antenna $n$,

$I_m(0)$ current at input of antenna $m$,

$I_m{}^*$ complex conjugate of $I_m$,

$Z_{mn}$ mutual impedance of antenna $m$ due to current of antenna $n$.

From [5]

$$Z_{mn} = -\frac{1}{I_n(0) I_m{}^*(0)} \int_{-l/2}^{l/2} E_{mn}(Z)\cdot I_m{}^*(Z)\,dZ.$$

In Fig. 5, the ground plane is replaced by image dipole currents. The image currents are multiplied by the reflection coefficient $\rho$ of the medium. Then, $I_3 = \rho I_1$ and $I_4 = \rho I_2$. Equations (24) and (25) can be solved for the total terminal impedances of the transmit and receive dipoles, denoted $Z_{T_1}$ and $Z_{T_2}$, respectively. The receiving antenna is assumed to be terminated in 50 Ω ($Z_L = 50$ Ω). For a perfectly conducting

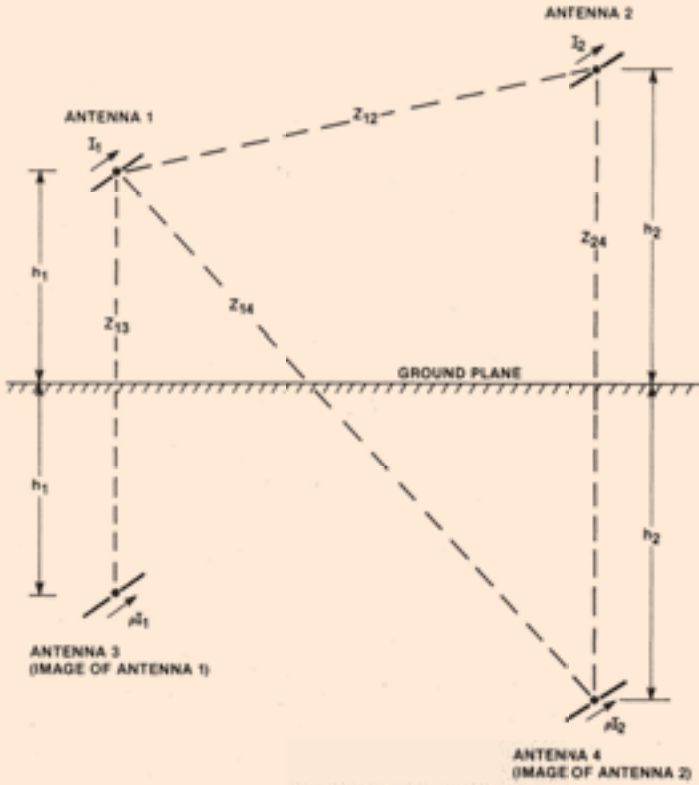


Fig. 5. Mutual-impedance geometry for two horizontally polarized dipole antennas over an infinite ground plane using the method of images.

ground plane, $\rho = -1$. Also, $Z_{23} = Z_{14}$ by symmetry (Fig. 5) and $Z_{12} = Z_{21}$ by reciprocity. We have

$$V_1 = I_1(Z_{11} - Z_{13}) + I_2(Z_{12} - Z_{14})$$

$$V_2 = I_1(Z_{12} - Z_{14}) + I_2(Z_{22} - Z_{24}) = -I_2 Z_L$$

$$Z_{T_1} = \frac{V_1}{I_1}$$

$$= Z_{11} - Z_{13} - \frac{(Z_{12} - Z_{14})^2}{(Z_{22} + Z_L - Z_{24})}$$

$$= Z_{11} + Z_m{}^1 \tag{26}$$

$$Z_{T_2} = \frac{V_2}{I_2} = Z_{22} - Z_{14} - \frac{(Z_{12} - Z_{14})^2}{(Z_{11} + Z_L - Z_{13})} = Z_{22} + Z_m{}^2 \tag{27}$$

where $Z_m{}^1$ and $Z_m{}^2$ are the total mutual impedances of antennas 1 and 2. The appropriate terminal impedance for each dipole antenna can thus be found for each geometry.

The solutions for the mutual impedances $Z_m$ of parallel cylindrical dipoles have been calculated by various authors [10]–[13]. The solutions for the infinitely thin case take the form of Si ($x$) and Ci ($x$) functions, where the following assumptions are made: 1) the self-impedances ($Z_{11}$ and $Z_{22}$) of the antennas remain constant; and 2) the current distribution along the antenna is sinusoidal. For relatively thin cylindrical dipoles, these assumptions yield adequate results.

The effect of mutual coupling on site attenuation can be accounted for by calculating the changes in the antenna factors of the transmit and receive antennas caused by their respective mutual impedances. (Since the transmit antenna is at a fixed height $h_1$ and the receive antenna is scanned over a height range $h_2{}^{\min} \leq h_2 \leq h_2{}^{\max}$, the mutual impedances of the two antennas will be different.)

The antenna factor for a dipole with self-impedance $Z_s = Z_{nn} = R_s + jX_s$ and total mutual impedance $Z_m = R_m + jX_m$ terminated in 50 Ω is

$$AF = \frac{50 + Z_s + Z_m}{50h}$$

where $h$ is the effective height. The isolated antenna factor ($Z_m = 0$) is

$$AF_0 = \frac{50 + Z_s}{50h}.$$

Let $\Delta AF$ denote the ratio of the antenna factor with mutual impedance to the isolated antenna factor. Then

$$\Delta AF = \frac{AF}{AF_0} = \frac{50 + Z_s + Z_m}{50 + Z_s}$$

and the magnitude, in decibels, is

$$\Delta AF\,(\text{dB}) = 10 \log \left[ \frac{(50 + R_s + R_m)^2 + (X_s + X_m)^2}{(50 + R_s)^2 + X_s{}^2} \right]. \tag{28}$$

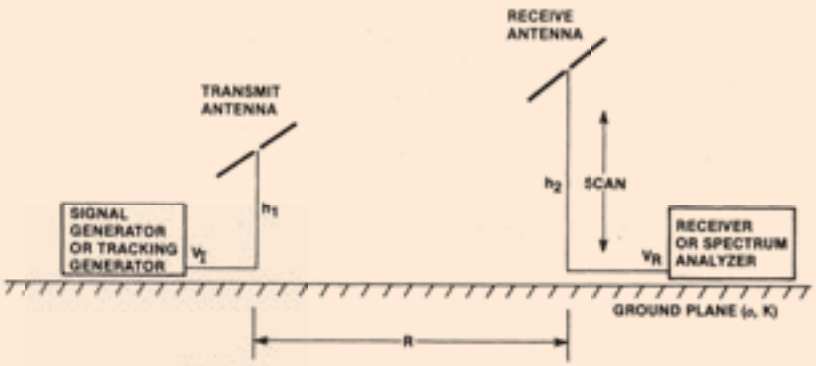


Fig. 6. Site-attenuation measurement procedure.

Equation (28) must be calculated separately for the transmit and receive antennas and added to each antenna factor term in (19) and (20) to account for mutual coupling. An illustration is given in Section IV.

## III. MEASUREMENT PROCEDURES

Two measurement procedures will be briefly described: a discrete-frequency method, and a swept-frequency method which requires a tracking generator and automatic spectrum analyzer, and which may be used with broad-band antennas (but not tunable dipoles).

The setup is common to both the discrete and swept methods. (Refer to Fig. 6.) The signal or tracking generator is connected to the transmit antenna with an appropriate length of transmission line. The transmit antenna is placed in the desired location, usually in the center of the area to be occupied by the equipment under test. Antenna height is set to $h_1$ and the desired polarization is selected. If a tunable dipole is used, the length is adjusted for the required frequency.

The receive antenna is mounted on a mast which allows scanning over the height range $h_2{}^{\min} \leq h_2 \leq h_2{}^{\max}$, placed at a distance $R$ from the transmit antenna, and connected to the field strength meter or spectrum analyzer. The appropriate polarization is selected and, if tunable, the antenna is adjusted to the required frequency. (Vertically polarized measurements below approximately 75 MHz are not practical with tunable dipoles because of their length.)

The following procedure is applicable to discrete frequency measurements. Tune the signal generator to the required frequency and adjust the output to a level which gives a received voltage well above ambient and receiver noise. Record the signal-generator output voltage level $V_I$. Scan the receive antenna over the height range $h_2{}^{\min} \leq h_2 \leq h_2{}^{\max}$ and record the maximum received voltage $V_R$. Repeat for the remaining discrete frequencies. Measure the total cable loss $C_A$ (transmit and receive cables) at each frequency. If cable loss is to be subtracted from the measured data (the preferred method), measured site attenuation is calculated as

$$A\ (\text{dB}) = V_I\ (\text{dB} \cdot \mu\text{V}) - V_R\ (\text{dB} \cdot \mu\text{V}) - C_A\ (\text{dB})$$

and the corresponding theoretical site attenuation is given by (19). If cable loss is to be added to the theoretical site attenuation, measured site attenuation is calculated from

$$A\ (\text{dB}) = V_I\ (\text{dB} \cdot \mu\text{V}) - V_R\ (\text{dB} \cdot \mu\text{V})$$

and the corresponding theoretical site attenuation is given by (20).

The following procedure is applicable to swept-frequency measurements. Adjust the output level of the tracking generator to give a received-voltage spectrum well above ambient and receiver noise. Raise the receiving antenna on the mast to the maximum height of the scan range $h_2{}^{\max}$. Set the automatic spectrum analyzer to sweep the desired frequency range and place in MAX HOLD. Slowly lower the receiving antenna to the minimum height of the scan range $h_2{}^{\min}$. Store the maximum-received-voltage spectrum in register $B$ of the spectrum analyzer. Disconnect the transmit and receive cables from the antennas and connect the two cables with a straight adapter. Store the cable-loss spectrum in register $A$ of the spectrum analyzer. Subtract the contents of register $B$ from the contents of register $A$ and store the result in $A$ (i.e., depress the button $A - B \rightarrow A$). The measured site attenuation is stored in register $A$ and may be plotted on an $x$-$y$ plotter. (See, for example, Figs. 7-12, 16, 17. The measured curves in these figures are tracings of actual spectrum-analyzer $x$-$y$ plotter outputs.) The corresponding theoretical site attenuation is given by (19).

Variations in the above procedures may be necessary, depending on available test-equipment characteristics.

The measurements in the following sections were made with a Hewlett-Packard HP 8581A Automatic Spectrum Analyzer. An HP8640B Signal Generator was used for discrete-frequency measurements, and an HP 8444A Tracking Generator for swept-frequency measurements. A Schwarzbeck AM 9104 Antenna Mast was used to scan the receiving-antenna height.

## IV. COMPARISON OF MEASURED AND THEORETICAL RESULTS

Measured and theoretical site attenuations are compared in Figs. 7-17 for a variety of sites, antennas, and geometries ($h_1$, $h_2$, $R$) for both horizontal and vertical polarizations. All theoretical curves in these figures were calculated from either (19) or (20), depending on how cable loss was accounted for.

Figs. 7-10 show measured and calculated site attenuations at a distance of 10 m over a conducting plane using broad-band antennas in the frequency range 30-1000 MHz for both horizontal and vertical polarizations. Biconical dipoles were used from 30 to 200 MHz and log planar antennas from 200 to 1000 MHz. Measurements were made using the swept-frequency method described in Section III. (Ambient

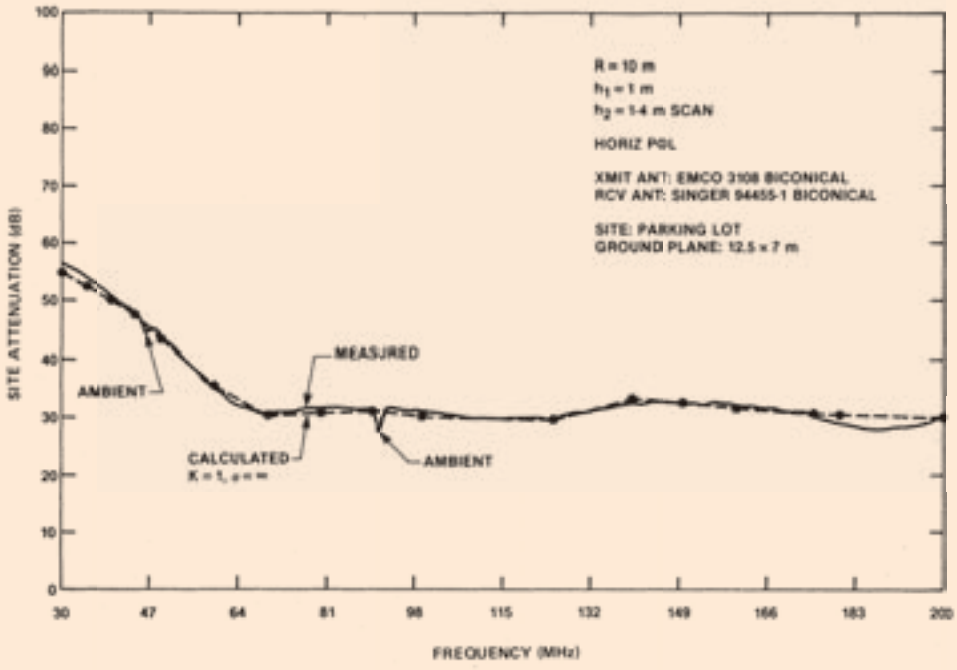


Fig. 7. Horizontal site attenuation for 10 m over a conducting plane using broad-band antennas, 30–200 MHz.

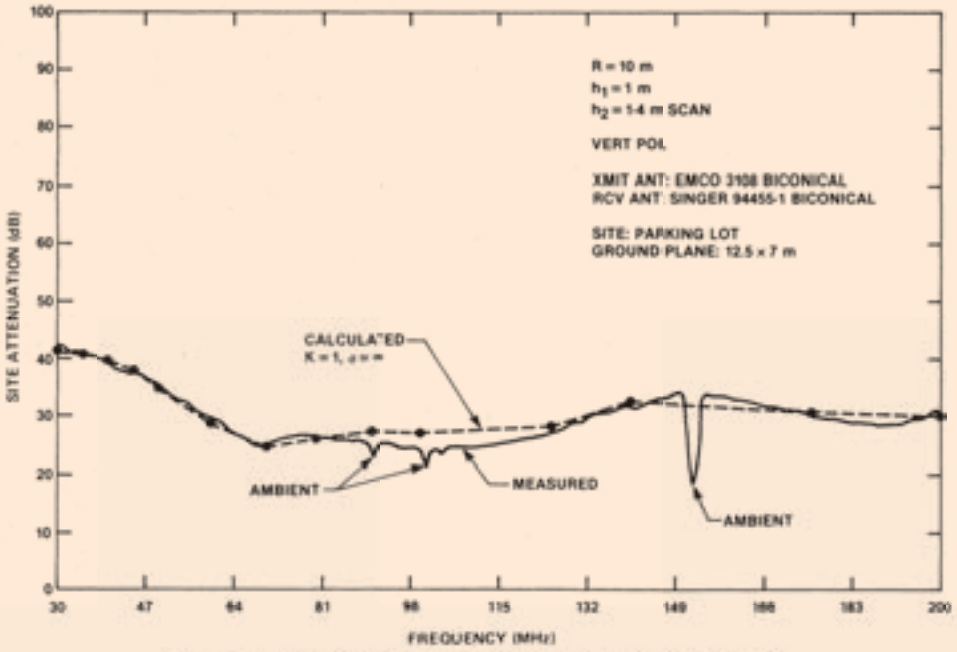


Fig. 8. Vertical site attenuation for 10 m over a conducting plane using broad-band antennas, 30–200 MHz.

signals show up as nulls on the measured curves, since the received-voltage spectrum is subtracted from the cable-loss spectrum to obtain the measured site-attenuation spectrum plot.) These figures show excellent agreement between measured and theoretical site attenuations (within 3 dB over most of the frequency range and within 4 dB at 1000 MHz).

Measured and calculated site attenuations at a distance of 3 m over a conducting plane using broad-band biconical dipoles in the frequency range 30–200 MHz are compared in Figs. 11 and 12 for horizontal and vertical polarizations, respectively. The dip in measured site attenuations around 190 MHz in both figures is attributed to a dip in the antenna factor of one of the antennas. (This dip is also evident in Figs. 7 and 8.) Measured antenna factors for these antennas at 190 MHz were not available for inclusion in the theoretical model.

The antenna heights in Figs. 7–12 were selected following

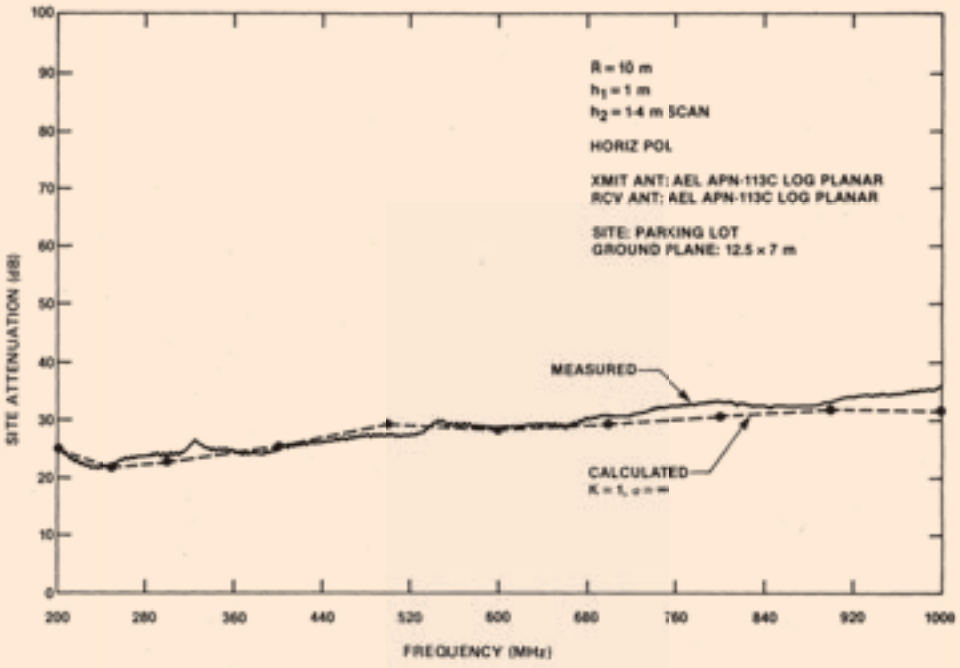


Fig. 9. Horizontal site attenuation for 10 m over a conducting plane using broad-band antennas, 200–1000 MHz.

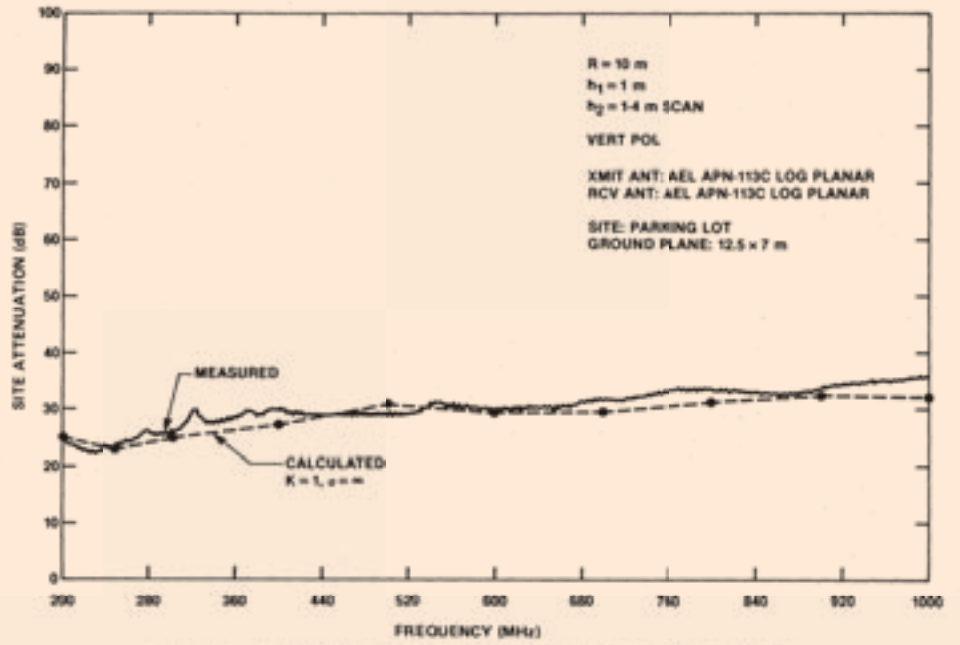


Fig. 10. Vertical site attenuation for 10 m over a conducting plane using broad-band antennas, 200–1000 MHz.

the guidelines in [14]. The results in Figs. 7–12 show that site-attenuation measurements can be made using geometries representative of actual EMC measurements on products. Note that Figs. 7 and 11 differ by 10 dB, which is consistent with inverse-distance fall-off between 3 and 10 m.

Fig. 13 shows discrete-frequency horizontal site-attenuation measurements at a distance of 30 m over earth using two identical broad-band cylindrical dipoles. The theoretical site attenuation curve calculated from the manufacturer's antenna factor deviates considerably from the measured curves, due to errors in the manufacturer's antenna factor. (Since the transmit and receive antenna factor errors are additive in (19) and (20), the antenna factor error for the two identical antennas in Fig. 13 is approximately *one-half the difference* between measured and calculated curves.) All of the antennas used in this study, including two different tunable dipoles, exhibited

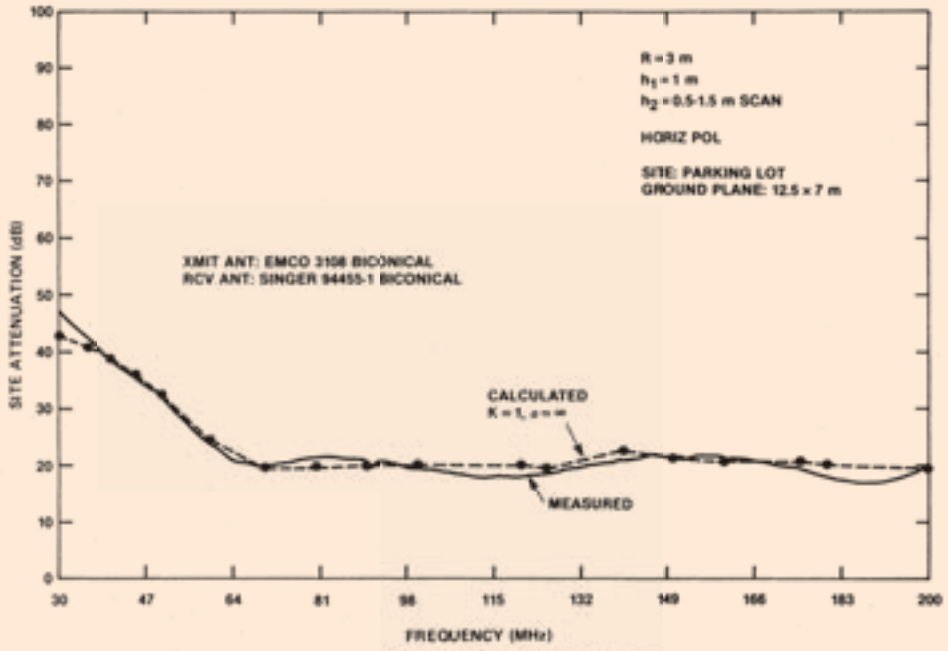


Fig. 11. Horizontal site attenuation for 3 m over a conducting plane using broad-band antennas, 30–200 MHz.

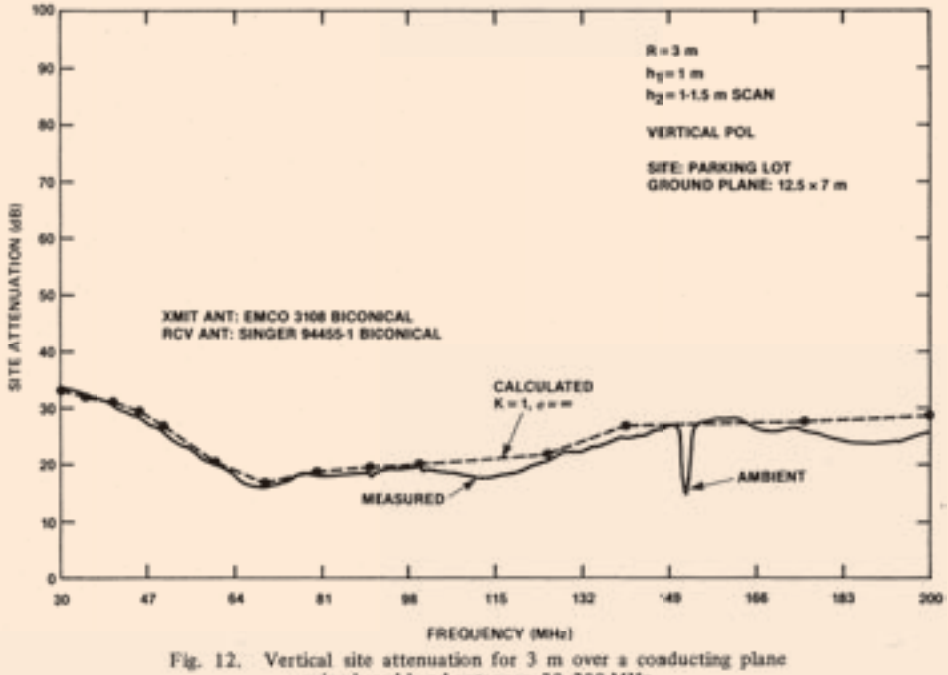


Fig. 12. Vertical site attenuation for 3 m over a conducting plane using broad-band antennas, 30–200 MHz.

similar errors in manufacturers' antenna factors. For this reason, a set of tunable dipoles was sent to the National Bureau of Standards for calibration, then used as a secondary standard to measure the antenna factors of the antennas used for site-attenuation measurements. The calculated site-attenuation curve in Fig. 13 using the measured antenna factors agrees quite closely with the measured site attenuation.

Horizontal site attenuation using tunable dipoles at a distance of 30 m over earth is shown in Fig. 14. No mutual coupling effects at the low frequencies are evident at a distance of 30 m.

Fig. 15 shows horizontal site-attenuation data for tunable dipoles at a distance of 3 m over a conducting plane. The extent of mutual coupling effects between horizontally-polarized tuned dipoles at a separation of 3 m can be assessed by comparing the measured site attenuation with the site-attenuation curve calculated from (20) with no mutual-impedance correction. At 30 MHz, the difference between these curves is 3.6

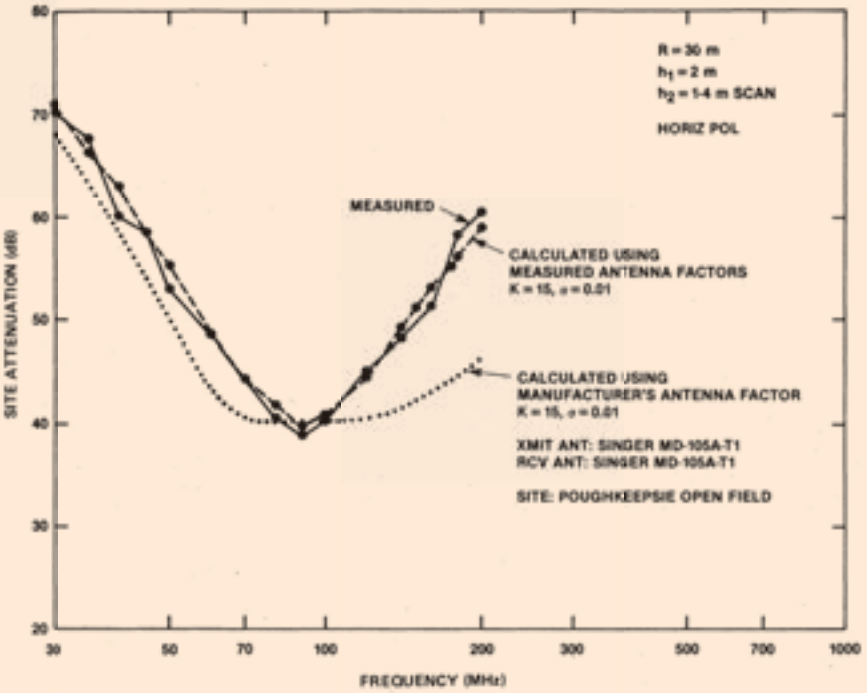


Fig. 13. Horizontal site attenuation for 30 m over earth using broad-band dipoles.

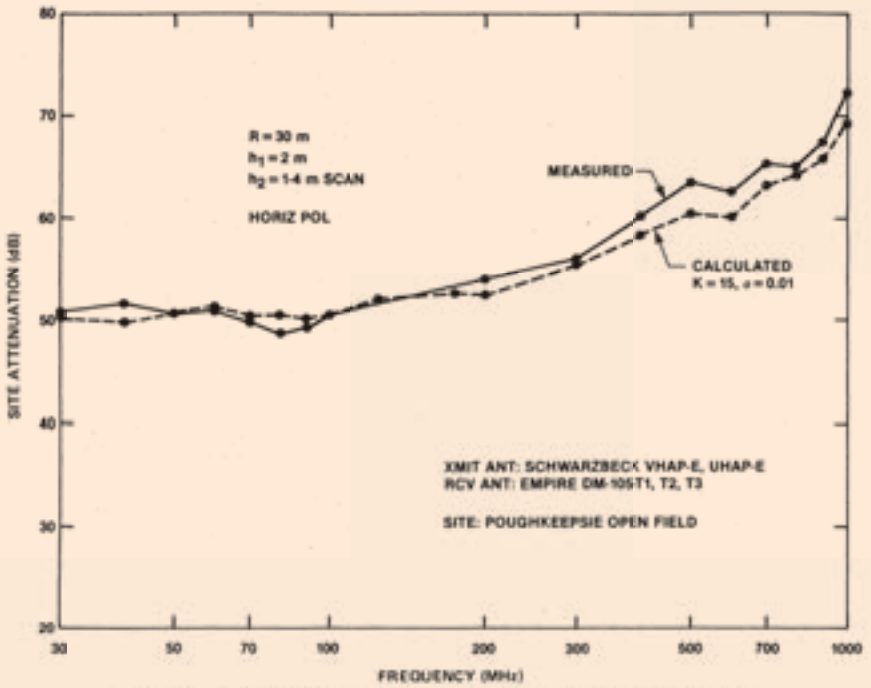


Fig. 14. Horizontal site attenuation for 30 m over earth using tunable dipoles.

dB. (Mutual coupling effects between horizontally-polarized broad-band biconical antennas separated by 3 m are also evident in Fig. 11. At 30 MHz, the difference between measured and uncorrected theoretical site-attenuation curves is 4 dB, compared with 3.6 dB for the tunable dipoles in Fig. 15. The broad-band dipoles in Fig. 11 are, however, much closer to the ground plane than the tuned dipoles in Fig. 15, i.e., $h_1 = 1$, $h_2 = 0.5$–$1.5$ versus $h_1 = 2$, $h_2 = 1$–$4$. Under the same geometry, the shorter broad-band dipoles would exhibit less mutual coupling than tuned dipoles.) When the tuned-dipole antenna

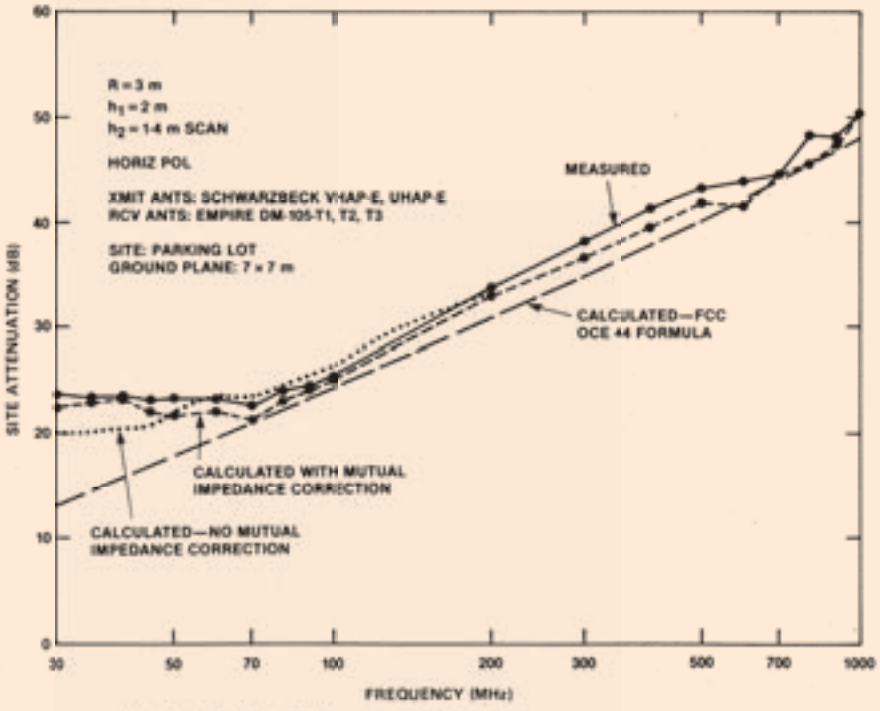


Fig. 15. Horizontal site attenuation for 3 m over a conducting plane using tunable dipoles.

factors are corrected for mutual coupling by adding (28) to (20), excellent agreement between measured and calculated site attenuations is obtained, as shown in Fig. 15. See Appendix IV for the numerical mutual-coupling data for the antennas and geometry in Fig. 15.

The theoretical site attenuation curve proposed in FCC Bulletin OCE 44 [3] is also plotted in Fig. 15. The difference between the OCE 44 curve and the measured site attenuation at 30 MHz is approximately 10.5 dB. A brief analysis shows that this 10.5-dB difference is due to three factors: 3.5 dB from neglecting mutual coupling, 3.5 dB from incorrectly accounting for the magnitude and phase of the ground-reflected wave (i.e., by assuming a 4.7-dB average ground-reflection factor), and approximately 3.5 dB due to antenna losses (which are included in the antenna factors but not the FCC formula, which assumes lossless matched dipoles).

Two applications of site-attenuation measurements to the characterization of non-open-field measurement sites are shown in Figs. 16 and 17. The measured site attenuation for a semianechoic chamber in the range 25 to 200 MHz is given in Fig. 16. Broad-band cylindrical dipoles were used at a distance of 3 m. The theoretical open-field curve from (19) is shown for comparison.

Horizontal site-attenuation measurements made in a large factory site from 30 to 200 MHz using broad-band antennas separated by 10 m are given in Fig. 17. The theoretical open-field curve is also shown. The comparable open-field site attenuation using the identical geometry and antennas is given in Fig. 7.

The graduation from open-field to anechoic chamber to factory site reveals an increase in reflections, but surprisingly less than expected. It is interesting to note that, generally, the fields inside an anechoic chamber or a building are higher than the fields on an outdoor site. That is, indoor site-attenuation measurements are generally lower than outdoor site-attenuation measurements. It is conjectured that this effect results mainly from the contribution of ceiling-reflected waves. Compare, for instance, the outdoor measurement in Fig. 7 with the indoor measurements in Figs. 16 and 17.

## V. DISCUSSION

Comparison of our measured and calculated site attenuations for open-field sites reveals a maximum difference of approximately 4 dB. Generally, the results were much closer. Most of this difference is attributed to antenna-factor inaccuracies. The antenna factors of the antennas we used were measured against a set of tunable dipoles calibrated by the National Bureau of Standards (NBS) in Boulder, CO. NBS estimates that the uncertainty of the antenna factors of the tunable dipoles is ±1 dB. At least another ±1-dB uncertainty was added during the calibration of our test antennas against the NBS calibrated tunable dipoles. Since two antennas are used for site attenuation measurements, the total uncertainty is in the order of ±4 dB, which is consistent with our results.

Use of manufacturers' published antenna factors will generally result in greater differences betweeen measured and calculated site attenuations than we obtained with calibrated antennas. We found that errors in manufacturers' antenna factors ranged from 1.5 to 6 dB, depending on the particular antenna. Surprisingly, the antenna factors of tunable dipoles

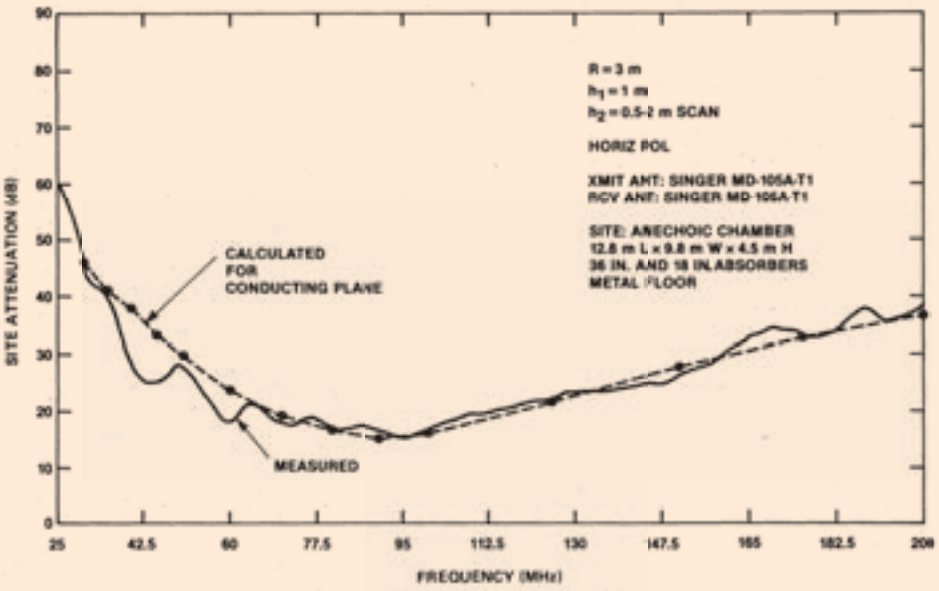


Fig. 16. Horizontal site attenuation for 3 m in a semianechoic chamber using broad-band antennas.

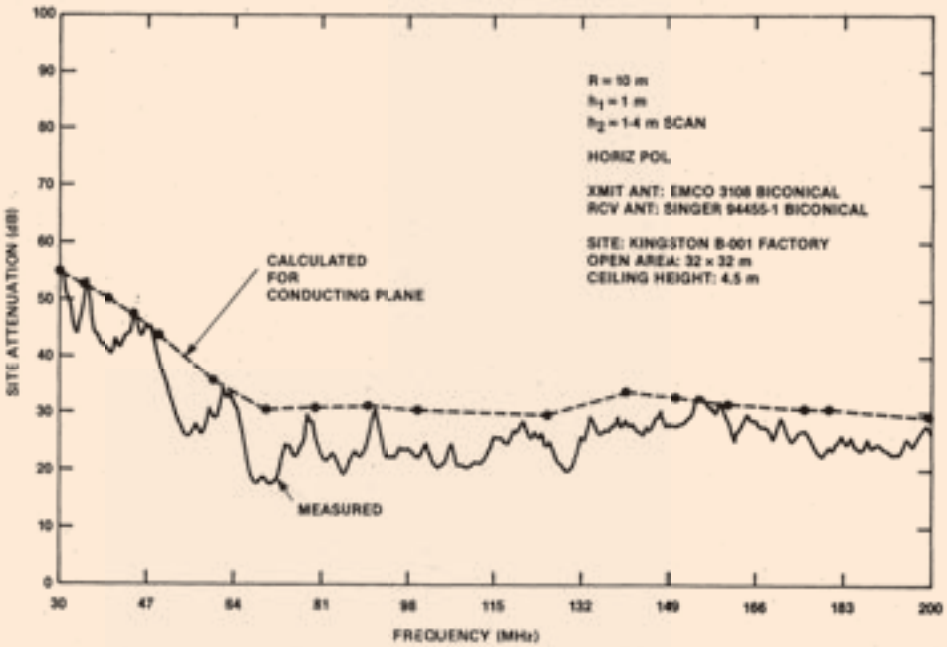


Fig. 17. Horizontal site attenuation for 10 m in a factory using broad-band antennas, 30–200 MHz.

were found to be no more accurate than those of most of the broad-band dipoles.

We found that vertical-polarization site-attenuation measurements were stable and repeatable, and no more subject to error than horizontal measurements. This contrasts with the results of Bennett and Taggart [7]. They found that measurements of vertically polarized waves in the far-field over a conductive ground screen using fixed antenna heights were erratic and often not repeatable to within 10 dB. This difference in conclusions is attributed to the use of antenna-height scanning for site-attenuation measurements, which eliminates sensitivity to nulls.

Our results revealed no significant mutual coupling effects between vertical antennas and their transmission lines. Our results also failed to show any significant effects due to scattering from the transmission lines or nonuniform illumination of vertical antennas at close separations as hypothesized by Dvorak and Meyer [15].

Mutual-coupling effects are evident for closely-spaced horizontally-polarized antennas. While more pronounced for tunable dipoles (see Fig. 15), broad-band biconicals also exhibit mutual coupling at a 3-m spacing for lower antenna heights, e.g., see Fig. 11, where $h_1 = 1$ and $h_2 = 0.5$–$1.5$ m. (Mutual-coupling effects are negligible for vertically polarized antennas.)

The error caused by neglecting mutual coupling for the geometries we examined is approximately 3 to 4 dB at 30 MHz, which is the same order of error resulting from antenna-factor uncertainties at higher frequencies. If a tolerance on the order of ±7 dB is acceptable for combined site and antenna errors, then mutual-coupling corrections could be neglected in the calculations, considerably simplifying the computational effort. (A tolerance of approximately ±7 dB seems reasonable based on a ±4-dB antenna-factor uncertainty as discussed above and a ±3-dB site deviation, allowed for example by the IEC [4].)

An approximate approach for handling mutual-coupling effects for horizontally polarized tuned dipoles at a 3-m spacing would be to add a correction factor which varies linearly from 4 dB at 30 MHz to 0 dB at 60 MHz, regardless of actual antenna heights. While only an approximation, this would avoid recomputing mutual impedances for each set of antenna heights ($h_1$, $h_2$) and certainly would result in better agreement than neglecting mutual coupling. (Applying this approximate correction to the calculated curve with no mutual-coupling correction in Fig. 15 results in reasonably good agreement.) A similar rule-of-thumb correction for biconicals (or other broad-band antennas approximately 2 m in length) with low antenna heights (e.g., $h_1 = 1$, $h_2 = 0.5$–$1.5$) would vary linearly from 4 dB at 30 MHz to 0 dB at 40 MHz. Broad-band antennas with greater heights (e.g., $h_1 = 2$, $h_2 = 1$–$4$) exhibited no mutual-coupling effect.

## VI. CONCLUDING REMARKS

A model has been developed for calculating site attenuation in terms of the antenna factors of the transmit and receive antennas and a ground-wave field-strength term. The model admits to both horizontal and vertical polarizations over earth or a conducting ground plane, and accounts for mutual-coupling effects between closely spaced horizontal dipoles. The validity of the theoretical model has been established by experimental results for a variety of sites, antennas, and geometries.

Expressing site attenuation in terms of antenna factors allows the use of broad-band antennas with their host of advantages over tunable dipoles. Specifically, tunable dipoles are restricted to discrete-frequency measurements requiring time-consuming adjustments of the antenna arms. The size of tunable dipoles at low frequencies (below approximately 75 MHz) makes them unsuitable for vertical-polarization measurements and precludes their use in most semianechoic chambers. Broad-band antennas, on the other hand, are compatible with automated instrumentation, and permit swept measurements over a large frequency range, resulting in a significant reduction in test time compared to tunable dipoles. Since they are shorter than tunable dipoles, broad-band antennas exhibit less mutual coupling and can be used for vertical-polarization measurements and in all semianechoic chambers.


Fig. 18. Antenna receiving an electric field.

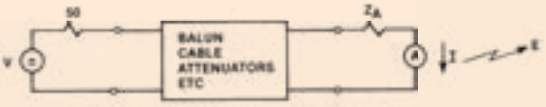


Fig. 19. Same antenna in transmitting mode.

Site attenuation is a measure of both the quality of the site and the accuracy of the transmit and receive antenna factors. Our results show that a comparison of measured and theoretical site attenuations for reasonably good open-field sites is primarily a measure of antenna-factor errors.

In addition to measuring site quality and antenna-factor accuracy, it may be possible to use site attenuation as a basis for correlating EMI measurements made on alternate sites to an ideal open-field site. This application requires further study.

## APPENDIX I
## TRANSMITTING ANTENNA CURRENT IN TERMS OF THE ANTENNA FACTOR

Refer to Fig. 18 which shows an antenna receiving an electric field $E$. The received voltage is $V_R$. By the definition of antenna factor

$$V_R = \frac{E}{AF}. \tag{I-1}$$

Since effective height $h$ is defined by $V = hE$, (I-1) can also be written as

$$V_R = \frac{V}{hAF}.$$

The current in the 50-Ω termination is

$$I = \frac{V_R}{50} = \frac{V}{50hAF}.$$

But, as shown in Appendix II

$$h = \frac{\lambda}{\pi}\left(\frac{GR_A}{120}\right)^{1/2}.$$

Then

$$I = \frac{V}{50AF}\,\frac{\pi}{\lambda}\left(\frac{120}{GR_A}\right)^{1/2}.$$

Invoking the reciprocity theorem, we interchange the ammeter $A$ and voltage source $V$ in Fig. 18, arriving at Fig. 19, which shows the antenna in the transmit mode. In Fig. 19, $V$ is now the open-circuit voltage of the signal generator, and $I$ is the antenna current. Evidently

$$I = \frac{V}{50AF_T}\,\frac{\pi}{\lambda}\left(\frac{120}{GR_A}\right)^{1/2}$$

TABLE I

| POLARIZATION | HORIZ | HORIZ | HORIZ | HORIZ | VERT | VERT | VERT | VERT |
|---|---|---|---|---|---|---|---|---|
| R meters | 3 | 10 | 30 | 30 | 3 | 10 | 30 | 30 |
| $h_1$ meters | 1 | 1 | 1 | 2 | 1 | 1 | 1 | 2 |
| $h_2$ meters | 0.5-1.5 | 1-4 | 1-4 | 1-4 | 1-1.5 | 1-4 | 1-4 | 1-4 |
| PLANE | METAL | METAL | EARTH | EARTH | METAL | METAL | EARTH | EARTH |
| f MHz | | | $E_D^{max}$ | dBuV/m | | | | |
| 30 | 1.6 | -10.4 | -26.9 | -21.8 | 11.2 | 2.7 | -14.7 | -13.8 |
| 35 | 2.7 | - 9.1 | -25.9 | -20.7 | 11.1 | 2.7 | -14.7 | -13.8 |
| 40 | 3.7 | - 8.0 | -25.0 | -19.7 | 11.1 | 2.7 | -14.7 | -13.8 |
| 45 | 4.6 | - 7.0 | -24.2 | -18.8 | 11.0 | 2.7 | -14.7 | -13.8 |
| 50 | 5.3 | - 6.1 | -23.5 | -18.0 | 10.9 | 2.6 | -14.7 | -13.8 |
| 60 | 6.7 | - 4.7 | -22.1 | -16.6 | 10.7 | 2.6 | -14.7 | -13.7 |
| 70 | 7.8 | - 3.5 | -21.0 | -15.4 | 10.5 | 2.6 | -14.7 | -13.6 |
| 80 | 8.8 | - 2.4 | -19.9 | -14.4 | 10.3 | 2.6 | -14.6 | -13.5 |
| 90 | 9.6 | - 1.6 | -19.0 | -13.5 | 10.0 | 2.5 | -14.5 | -13.4 |
| 100 | 10.2 | - 0.8 | -18.1 | -12.6 | 9.6 | 2.5 | -14.5 | -13.3 |
| 120 | 11.2 | 0.4 | -16.7 | -11.3 | 8.8 | 2.4 | -14.5 | -13.1 |
| 125 | 11.4 | 0.6 | -16.3 | -11.0 | 8.6 | 2.4 | -14.3 | -13.0 |
| 140 | 11.9 | 1.2 | -15.4 | -10.2 | 7.8 | 2.3 | -14.1 | -12.8 |
| 150 | 12.1 | 1.5 | -14.9 | - 9.8 | 7.2 | 2.3 | -14.0 | -12.7 |
| 160 | 12.2 | 1.8 | -14.3 | - 9.3 | 6.5 | 2.2 | -13.9 | -12.6 |
| 175 | 12.3 | 2.1 | -13.6 | - 8.8 | 5.4 | 2.1 | -13.8 | -12.4 |
| 180 | 12.4 | 2.1 | -13.4 | - 8.6 | 5.0 | 2.1 | -13.7 | -12.4 |
| 200 | 12.5 | 2.3 | -12.6 | - 8.1 | 3.2 | 1.9 | -13.5 | -12.2 |
| 250 | 12.7 | 2.5 | -10.9 | - 7.3 | 7.2 | 1.5 | -13.0 | -11.7 |
| 300 | 12.7 | 2.6 | - 9.7 | - 7.1 | 9.7 | 0.9 | -12.5 | -11.4 |
| 400 | 12.8 | 2.7 | - 9.0 | - 7.0 | 10.9 | 1.0 | -11.7 | -10.8 |
| 500 | 12.8 | 2.8 | - 7.2 | - 7.0 | 11.3 | 1.7 | -11.2 | -10.5 |
| 600 | 12.5 | 2.8 | - 7.0 | - 6.9 | 9.5 | 2.0 | -10.7 | -10.2 |
| 700 | 12.6 | 2.8 | - 7.0 | - 6.9 | 10.4 | 2.2 | -10.4 | -10.0 |
| 800 | 12.7 | 2.8 | - 6.9 | - 6.9 | 10.9 | 2.4 | -10.1 | - 9.9 |
| 900 | 12.7 | 2.6 | - 6.9 | - 6.9 | 11.2 | 2.4 | - 9.9 | - 9.8 |
| 1000 | 12.8 | 2.7 | - 6.9 | - 6.9 | 11.3 | 2.5 | - 9.7 | - 9.7 |

where $AF_T$ denotes the antenna factor of the antenna used for transmission in site-attenuation measurements.

## APPENDIX II
## EFFECTIVE HEIGHT OF A RECEIVING ANTENNA

The power $P_R$ received by a matched lossless antenna is equal to the product of the power density $W_T$ of the incident field and the maximum effective aperture $A_m$ [11]. That is

$$P_R = W_T A_M = \frac{E^2}{120\pi}\frac{\lambda^2 G}{4\pi}.$$

The voltage across the load $V_R$ is

$$V_R = \sqrt{P_R R_A} = \frac{E\lambda}{2\pi}\left(\frac{GR_A}{120}\right)^{1/2}$$

where $R_A$ is the load resistance (equal to the antenna radiation resistance). The open-circuit voltage of the antenna $V_{oc}$ is twice the received voltage, i.e.,

$$V_{oc} = \frac{E\lambda}{\pi}\left(\frac{GR_A}{120}\right)^{1/2}.$$

But the effective height $h$ is defined by

$$V_{oc} = hE.$$

Thus

$$h = \frac{\lambda}{\pi}\left(\frac{GR_A}{120}\right)^{1/2}.$$

The effective height $h$ is independent of the antenna load impedance, i.e., it is defined as the ratio of the open-circuit voltage to the incident electric field.

TABLE II

| f MHz | $Z_m^{XMIT}$ | $Z_m^{RCV}$ | $\Delta AF^{XMIT}$ dB | $\Delta AF^{RCV}$ dB | $\Delta AF^{TOT}$ dB |
|---|---|---|---|---|---|
| 30 | 1.2 + j55.0 | 12.2 + j4.6 | 1.7 | 0.8 | 2.5 |
| 35 | 23.9 + j39.4 | 10.7 - j3.4 | 2.2 | 0.7 | 2.9 |
| 40 | 31.5 + j17.9 | 9.2 - j11.2 | 2.1 | 0.7 | 2.8 |
| 45 | 26.3 + j1.6 | -3.0 - j8.0 | 1.6 | -0.2 | 1.4 |
| 50 | 20.1 - j7.0 | -15.0 - j4.9 | 1.1 | -1.2 | -0.1 |
| 60 | 8.4 - j20.4 | -20.9 - j16.0 | 0.2 | -1.6 | -1.4 |
| 70 | -8.6 - j14.5 | -20.0 - j12.7 | -0.9 | -1.5 | -2.4 |
| 80 | -12.0 - j2.7 | -8.9 - j7.6 | -0.9 | -0.6 | -1.5 |
| 90 | -6.3 - j0.5 | -6.1 - j3.1 | -0.4 | -0.4 | -0.8 |
| 100 | -8.4 + j2.2 | -7.8 - j11.2 | -0.5 | -0.5 | -1.0 |
| 150 | -1.9 - j12.4 | -9.9 - j11.8 | -0.4 | -0.7 | -1.1 |
| 200 | 7.4 + j1.8 | -3.7 - j1.8 | 0.5 | -0.3 | 0.2 |

## APPENDIX III
## TABULATIONS OF $E_D^{max}$ FOR SOME TYPICAL GEOMETRIES

The values of $E_D^{max}$ listed in Table I were calculated from (8) and (13) for the indicated geometries using $K = 15$, $\sigma = 0.01$ for earth ground planes and $K = 1$, $\sigma = \infty$ for metal ground planes.

## APPENDIX IV
## MUTUAL-IMPEDANCE CORRECTION FOR THEORETICAL SITE ATTENUATION IN FIG. 15

Table II lists the calculated mutual impedances and antenna-factor corrections for the half-wavelength transmitting dipole ($Z_S = 73 + j42$) and resonant receiving dipole ($Z_S =$

70 + $j0$) in Fig. 15 for the geometry $R = 3, h_1 = 2, h_2 = 1$–4. Mutual impedances were calculated as described in Section II-F, and antenna-factor corrections were calculated from (28).

## ACKNOWLEDGMENT

The authors wish to thank A. C. Masch, P. F. McCarthy, K. M. Soo Hoo, and M. M. Truex of the IBM Poughkeepsie EMC Laboratory for their valuable help in the measurement effort, which covered numerous sites and took place under sometimes arduous conditions.

## REFERENCES

[1] C. R. Burrows, "Radio propagation over plane earth—Field strength curves," *Bell Syst. Tech. J.*, vol. 12, pp. 45–75, Jan. 1937.

[2] H. T. Friis, "A note on a simple transmission formula," *Proc. IRE.*, pp. 254–256, May 1946.

[3] Federal Communications Commission, "Calibration of a radiation measurement site—Site attenuation," docket 21371, appendix A, bulletin OCE 44, Sept. 9, 1977.

[4] "Recommended methods of measurement of radiated and conducted interference from receivers for amplitude modulation, frequency-modulation, and television broadcast transmissions," 2nd ed., IEC Pub. 106, 1974.

[5] T. Kawana and S. Miyajima, "Theoretical investigations on site attenuation—Propagation characteristics inside the measuring site for the radio interference," *J. Radio Res. Lab. Jap.*, vol. 25, no. 117/118, pp. 105–115, July/Nov. 1978.

[6] T. Kawana and S. Miyajima, "Theoretical investigations of site attenuation by means of mutual impedance between antennas," in *3rd Symp. Technical Exhibit. EMC*, (Rotterdam) May 1–3, 1979, pp. 83–88.

[7] W. S. Bennett and H. E. Taggart, "Characterization of a cispr/vde far-field emi test site with ground screen," in *3rd Symp. Technical Exhibit. EMC*, (Rotterdam) May 1–3, 1979, pp. 507–513.

[8] W. S. Bennett, "Ground plane effects on far-field emi measurements," *IEEE Int. Sym. EMC*, (San Diego, CA) Oct. 9–11, 1979, pp. 365–368.

[9] K. Bullington, "Radio propagation at frequencies above 30 megacycles," *Proc. IRE*, pp. 1122–1136, Oct. 1947.

[10] S. Schelkunoff and H. Friis, *Antennas, Theory and Practice*. New York: Wiley, 1952, pp. 407–412.

[11] J. Kraus, *Antennas*. New York: McGraw Hill, 1950, pp. 254–272, pp. 41–55.

[12] R. W. P. King, H. R. Mimno, and A. H. Wing, *Transmission Lines, Antennas, and Waveguides*. New York: Dover, 1965, pp. 125–130.

[13] C. T. Tai, "Coupled antennas," *Proc. IRE*, pp. 487–500, April, 1948.

[14] R. F. Germar and R. Calcavecchio, "On radiated emi measurement in the vhf/uhf frequency range," *IEEE Int. Symp. EMC*, (Baltimore, MD) Oct. 7–9, 1980, pp. 91–97.

[15] T. Dvorak and G. Meyer, "Influence of ground reflection in open site measurements of broadband interference," *IEEE Int. Symp. EMC*, (San Diego, CA) Oct. 9–11, 1979, pp. 369–374.

EMC